Hybrid MILP–GA–RL Framework for EV Charging Station Placement in Urban India

Tishya Jha[#1], Aarna Kuma[#2], Swez Bhardwaj[#3], Devisha Bhargava[#4], Shivam Shaurya[#5], Vishesh Gautam[#6]

[#]*Computer Science & Engineering Department, Rajiv Gandhi Institute of Petroleum Technology*
Jais, Uttar Pradesh, India

***Abstract*— The rapid growth of electric vehicle (EV) adoption in India has intensified the need for strategically planned charging infrastructure that balances user accessibility, economic feasibility, and power-grid reliability. However, most existing EV charging station placement models either assume uniform demand distributions or ignore critical real-world constraints such as grid-extension costs, heterogeneous urban demand patterns, and post-deployment operational performance. In this work, we develop a comprehensive, data-driven optimization framework for charging station deployment in the Lucknow urban core by integrating geospatial datasets, electricity-grid proximity, and EV adoption patterns. We construct a multi-objective mathematical model that minimizes driver detour, power-grid stress, and installation cost, while enforcing zone-specific coverage requirements. A refined demand model combines building density, commercial activity (POIs), and district-level EV sales, while restricting demand to four-wheeler vehicles to reflect practical infrastructure requirements. Power-grid distance is incorporated as a cost penalty to discourage infeasible siting. A small-scale MILP prototype validates the mathematical correctness of the model, and a scalable NSGA-II/GA implementation generates Pareto-optimal placement plans over 150–300 candidate locations. To address real-time operational efficiency, we integrate a Q-learning module that reduces charging wait times by dynamically routing vehicles to stations with minimal queue lengths. Baseline comparisons against random, uniform, and greedy placement strategies demonstrate substantial improvements in coverage, QoS, cost efficiency, and load balancing. The proposed hybrid methodology provides a robust planning and operational paradigm for data-driven EV infrastructure deployment in emerging urban regions.**

I. INTRODUCTION

The rapid electrification of road transport has created an urgent need for methodologically sound planning of electric vehicle (EV) charging infrastructure in emerging economies. Unlike conventional refuelling networks, EV charging infrastructures are tightly coupled to both the transportation layer (road network, traffic patterns, spatial distribution of activities) and the power-distribution layer (substations, feeders, grid capacity, voltage constraints). Planning decisions that ignore either dimension risk producing networks that are either underutilized, geographically inequitable, or economically infeasible due to excessive grid-extension costs. Existing literature on EV charging station siting has predominantly treated the problem as a variant of classical facility location, p-median, set-covering, or p-center optimization, occasionally extended by metaheuristic search for scalability. Parallel research streams address charger sizing, queueing and waiting-time minimization, and real-time routing as separate subproblems. This separation is analytically convenient but does not reflect the coupled nature of real deployments, where long-term siting and sizing decisions strongly interact with short-term operational routing and queue management. In particular, the spatial pattern of stations constrains the achievable performance of any real-time control or routing policy, while dynamic routing can, in turn, mitigate localized congestion created by suboptimal siting.

From a public-policy perspective, urban authorities must simultaneously answer at least three interacting questions: **Coverage:** Are all relevant zones within acceptable access distance of at least one station?
Quality of Service (QoS): Are stations placed preferentially where EV adoption and trip intensity are high, so as to minimize detour and waiting time for the majority of users?
Economic & Grid Feasibility: Are siting decisions aligned with the existing distribution network such that grid-extension costs and overload risks remain bounded?

Naïvely maximizing coverage by uniformly spreading stations may lead to severe underutilization in low-demand zones and unnecessary capital expenditure. Conversely, purely demand-driven siting may cluster stations in high-income or high-adoption neighborhoods, leaving peripheral regions underserved and contradicting equity and accessibility goals. Furthermore, a purely geographic or distance-based cost model fails to capture a critical real-world factor emphasized by practitioners: the distance from candidate station sites to the existing power grid infrastructure. Extending high-capacity feeders over long distances substantially increases capital cost, making some otherwise attractive locations economically unviable.

In this work, we focus explicitly on four-wheeler (4W) charging infrastructure, mirroring the emphasis of current government-built public fast-charging stations while acknowledging that e-rickshaw and two-wheeler charging require separate modelling and infrastructure design.

To capture these realities, we propose a data-driven formulation that integrates transportation, demand, and grid layers within a unified optimization framework. The study region is the Lucknow urban core, comprising dense commercial and residential neighborhoods with high potential for EV adoption. The region is modelled using: (i) an OpenStreetMap-derived road network, (ii) building footprints as a proxy for population and residential density, (iii) points of interest (POIs) such as malls, markets, office clusters, and transit hubs as proxies for trip-attraction intensity, (iv) district- or ward-level EV sales statistics as a proxy for adoption and purchasing capacity, and (v) distribution grid assets (substations, feeders) or their approximations to quantify grid proximity.

A. Coverage-Oriented versus QoS-Oriented Planning

A central conceptual refinement in this work is the explicit separation of coverage-oriented and QoS-oriented planning objectives.

In a coverage model, the planning objective is to guarantee that every zone (ward, grid cell, or policy-defined area) has at least one station within a specified maximum access distance. This is akin to classical

set-covering or p-center formulations, where the primary performance measure is whether demand points lie within a service radius of at least one facility and, optionally, the maximum or average distance to the nearest facility. Such a model is attractive to policymakers, as it provides clear guarantees of spatial equity: "no zone is left without access." In contrast, a QoS model seeks to optimize infrastructure primarily for areas with high EV demand and purchasing capacity. Here, station siting is driven by a composite demand score that combines (after appropriate scaling and normalization) built-up area or building footprint extent (proxy for population density), intensity of POIs (proxy for commercial and trip-attraction density), and EV sales or EV penetration indicators (proxy for local adoption potential). This composite demand is constructed as a weighted sum of normalized features,

$$D_i = w_B B_i + w_P P_i + w_E E_i$$

where $\tilde{B}_i, \tilde{P}_i, \tilde{E}_i \in [0,1]$ denote suitably normalized building area, POI density, and EV sales intensity at demand point i, and $w_B, w_P, w_E$are tunable hyperparameters. Rather than fixing these weights a priori, they are treated as tunable parameters and subjected to sensitivity analysis and/or simple hyperparameter search to ensure that the resulting station layouts are robust to reasonable changes in their values. This design choice avoids arbitrary reliance on a single assumed weighting scheme and allows the model to be calibrated to context-specific policy preferences—for example, prioritizing existing EV owners versus latent demand. Balancing coverage and QoS naturally leads to a multi-objective formulation. At one extreme, planners may require strict minimum coverage per zone (hard constraints) and then optimize QoS measures (detour, waiting time) within this feasible region. At the other extreme, they may wish to view coverage and QoS as competing objectives and explore the Pareto frontier of trade-offs. Our framework is designed to support both interpretations, either via a vector-valued objective,

$$\min\ (D(x), G(x), C(x)),$$

or via a weighted scalarization,

$$\min\ Z(x) = w_1 D(x) + w_2 G(x) + w_3 C(x),$$

where $D(x)$denotes aggregate detour, $G(x)$a grid-stress or grid-distance metric, and $C(x)$the total capital cost.

B. Grid Proximity and Economic Feasibility

A distinctive practical consideration in this work is the explicit incorporation of **distance to the existing power-distribution network** into the cost model. For each candidate station location k, we compute the shortest-distance metric $d_k^{\text{grid}}$to the nearest substation or feeder node, using the underlying geospatial representation of the distribution network. The installation cost at location $k$is then modelled as

$$Cost_k = C_0 + \alpha\, d_k^{\text{grid}},$$

where $C_0$is a base installation cost and $\alpha$is a grid-extension cost factor. This linear form is a first-order approximation that captures the key qualitative effect highlighted by practitioners: as one moves further from the existing grid backbone, the marginal cost of connecting a high-capacity charging station increases significantly. By embedding this term directly in the optimization model, the framework naturally discourages economically infeasible, grid-remote locations, even if they are attractive from a purely geometric or demand perspective.

This yields a more realistic design space in which feasible siting decisions emerge from a joint consideration of (i) demand intensity, (ii) coverage requirements, and (iii) proximity to the power grid. The model thereby provides a natural vehicle for exploring **cost–quality trade-off curves** (e.g., how much coverage and QoS can be obtained as the total budget increases, and at what marginal cost).

C. Long-Term Siting vs Short-Term Operations: MILP, GA, and Q-Learning

The resulting optimization problem—choosing which candidate locations to activate and how to assign spatially distributed demand to them, subject to coverage, capacity, budget, and grid distance constraints—is combinatorial and NP-hard. Mixed-Integer Linear Programming (MILP) provides a principled way to model this problem exactly, via binary siting variables, assignment variables, and linearized constraints capturing capacities and zone-based coverage. However, exact MILP quickly becomes computationally prohibitive as the number of candidate locations and demand points increases.

To reconcile model fidelity with computational scalability, we adopt a hybrid approach. A small-scale MILP prototype is first constructed over a reduced set of candidate sites and demand points. This prototype serves as a "ground truth" to validate the correctness of the mathematical formulation and to benchmark solution quality. For full-scale urban deployments with hundreds of candidate sites and demand centroids, we then employ a Genetic Algorithm (GA), specifically NSGA-II, which uses the MILP objective structure as its fitness evaluation. Each GA chromosome encodes a binary vector indicating which candidate locations are active; fitness evaluation assigns demand to open sites (via shortest-path detour on the road network), computes demand-weighted detour, grid-distance penalties, and total cost, and evaluates constraint satisfaction (coverage, capacity). NSGA-II then evolves a population of such solutions to approximate the Pareto front over detour, grid stress, and cost.

Even an optimally sited network does not guarantee low waiting times in practice, since EV arrivals are stochastic and temporally correlated (e.g., peak hours). To address the operational aspect, we overlay a simple yet effective Q-learning component on the optimized infrastructure. In this layer, the state encapsulates features such as current queue lengths and availability at nearby stations; actions correspond to routing an incoming EV to one of the reachable stations; and rewards penalize waiting time, queue length, and overload events. Through repeated interaction in a simulated environment, Q-learning converges to a policy that dynamically balances load among stations and reduces mean charging waiting time. This combination of GA-based strategic siting and RL-based operational control fills a gap in the literature, where the two have largely been treated independently.

D. Policy-Aware Zones and Benchmarking

To make the framework directly relevant for public planning, the study area is partitioned into policy zones (e.g., commercial hubs, residential belts, remote or underserved periphery). Each zone $z$is associated with a minimum coverage requirement $MinCoverage_z$, and constraints of the form

$$Coverage_z \geq MinCoverage_z$$

are imposed to prevent excessive clustering of stations in already well-served zones. This enables the exploration of policy configurations such as: (i) increased incentives for stations in remote or low-income zones, (ii) caps on the number of stations in saturated zones, and (iii) trade-offs between coverage guarantees and cost or QoS. Finally, to critically assess the benefits of the proposed optimization framework, we benchmark against several baseline strategies, including: random selection of candidate sites, uniform grid-based placement, and simple greedy schemes that iteratively select the highest-demand locations. These baselines provide intuitive "status quo" or "naïve planner" comparators for metrics such as coverage, average detour, total cost, and queue-based performance.

II. RELATED WORK

Research on EV charging infrastructure spans facility-location theory, MILP formulations, metaheuristic optimization, reinforcement-learning–based operational control, and policy-aware spatial planning. We summarize the most relevant directions below.

A. Station Placement

EV station siting is predominantly grounded in classical facility-location models such as p-median, p-center, set covering, and maximum coverage. These works minimize aggregate or worst-case travel distance over road networks, typically using population density, traffic volume, or OD flows as demand proxies. While computationally tractable, these models generally ignore heterogeneity across EV types, omit dynamic demand variations, and do not incorporate grid-proximity costs or zone-level policy constraints.

Thus, standard spatial optimization provides strong baselines but insufficient realism for deployment-grade planning.

B. MILP-Based Formulations

Mixed-Integer Linear Programming is widely used to encode station siting, charger sizing, capacity limits, and simplified grid constraints. MILP offers binary siting variables, charger-count decision variables, demand–facility assignment, and linearized coverage or power-flow restrictions.

However, MILP models scale poorly; realistic cities produce thousands of binary decisions and tens of thousands of assignment variables. Multi-objective variants (detour, cost, overload risk) further increase complexity. Consequently, MILP is mainly used on reduced instances for benchmarking or validation, motivating the need for scalable heuristics.

C. Metaheuristic Optimization

To address scalability, many studies adopt Genetic Algorithms (GA), PSO, ACO, Simulated Annealing, or hybrid variants. Typical features include binary chromosome encoding of station sites, multi-objective fitness functions (distance, cost, penalties), integration with network-based detour calculations, flexible handling of nonlinearities and constraint relaxations. Despite their flexibility, most metaheuristic approaches remain **static**: they optimize placement under assumed average demand and rarely incorporate: EV-adoption data, power-grid connection cost, socio-economic zoning, or dynamic queueing / waiting-time effects. Our work uses **NSGA-II** as the scalable optimizer but embeds richer demand, cost, and zoning models consistent with our MILP formulation.

D. Reinforcement Learning for EV Operations

Reinforcement Learning is extensively applied to operational problems rather than siting dynamic charging scheduling, load balancing and tariff response, queue management, routing drivers among existing stations. DRL methods (DQN, PPO, A2C, QL) optimize sequential decisions with states including queue lengths, loads, and price signals. However: RL is almost never used for long-term siting due to enormous state/action spaces, existing RL-siting prototypes operate only on small toy networks, grid constraints and true detour modelling are seldom embedded. Therefore, QL is best viewed as an operational optimizer complementing, not replacing, strategic facility location.

E. Policy & Zoning Approaches

A smaller literature explores equity, spatial disparity, and zoning regulations for EV infrastructure. These studies highlight issues such as clustering in profitable commercial zones, poor coverage in low-income or peripheral wards, the need for zone-specific service guarantees or subsidies. However, mathematical formulations incorporating explicit zone coverage constraints, EV affordability indicators, or EV adoption distributions remain limited. Policy-aware planning is typically qualitative rather than embedded in optimization. Our model formalizes zoning in the constraints, enabling explicit trade-offs between social equity and QoS.

F. Research Gaps

Synthesizing the strands above and our prior Stage-1/Stage-2 analysis, several gaps remain at the intersection of siting, grid constraints, demand modelling, and operations:

Fragmented treatment of siting, sizing, and operations, Limited integration of demand and adoption signals, Underrepresentation of grid-proximity effects in siting cost, Static metaheuristics without operational feedback, RL confined to operational control, not linked to siting, Insufficient policy-aware zoning models.

The present work addresses these gaps by (i) combining a MILP-structured, NSGA-II–based siting model with a Q-learning operational layer; (ii) using a multi-source, tunable demand model driven by buildings, POIs, and EV sales; (iii) embedding grid-distance–based cost penalties; and (iv) enforcing zone-specific coverage constraints to align optimization outcomes with policy objectives.

III. Preliminary Observations

The exploratory assessment of socio-economic, infrastructural, and spatial characteristics of the Lucknow urban core reveals several structural regularities that materially influence EV charging infrastructure design. These observations guide the modelling choices and justify the multi-objective formulation adopted in later sections.

A. Spatial Heterogeneity in EV Adoption and Purchasing Power

District- and ward-level EV sales distributions display strong spatial heterogeneity, with high-income commercial corridors (e.g., Gomti Nagar, Hazratganj) showing markedly higher 4W EV penetration than peripheral or low-income wards. EV adoption correlates with built-up density, POI concentration, and socio-economic indicators. Consequently, demand cannot be approximated by uniform population density; it must incorporate adoption intensity. This motivates the use of a composite demand index integrating normalized building density, POI density, and EV sales intensity.

B. Power-Grid Accessibility as a Dominant Cost Determinant

Preliminary overlays of the distribution network show significant variation in feeder and substation density across zones. The capital cost of installing a fast-charging hub rises sharply with increasing distance from grid infrastructure. Thus, a location's feasibility is

strongly influenced by its proximity to substations. A cost model incorporating a grid-distance penalty is therefore necessary to avoid economically impractical site selections and to ensure infrastructural viability.

C. Natural Emergence of Functional Zones

Spatial clustering of commercial POIs, residential buildings, and peri-urban characteristics produces clear functional zones within the study area. Absent zoning constraints, demand-driven optimizers disproportionately select sites in commercial cores, leading to over-concentration and undersupply in remote regions. This necessitates explicit zone-level coverage requirements to ensure equitable spatial distribution of infrastructure.

D. Clustering Tendencies of Pure QoS or Demand-Driven Objectives

Visualizations of demand surfaces reveal heavy concentration around a few commercial hubs, creating a skewed distribution that inherently biases optimization toward a small subset of candidate locations. A single-objective or purely QoS-driven formulation collapses onto these hotspots. The conflicting influences of demand intensity, grid accessibility, and spatial equity imply a multi-modal objective landscape, reinforcing the need for multi-objective optimization (e.g., NSGA-II) rather than scalarized decision rules.

E. Implications for the Siting Problem

Collectively, the observations indicate that:

- distance-minimizing formulations are insufficient due to nonuniform EV adoption and heterogeneous infrastructure accessibility;
- explicit zoning is required to prevent clustering and ensure equitable service;
- cost–quality trade-off analyses are essential for budget-sensitive planning;
- a hybrid architecture is required, with MILP validating small-scale structure, GA handling large-scale siting, and RL addressing post-deployment operational behavior.

These insights provide the empirical and conceptual motivation for the formal optimization framework described next.

IV. PROBLEM DEFINITION

We now formalize the EV charging station placement problem over the Lucknow urban core as a mixed-integer, multi-objective optimization model. The formulation jointly captures (i) coverage requirements across policy zones, (ii) quality-of-service (QoS) criteria related to driver detour and demand-weighted accessibility, and (iii) economic feasibility via a power-grid–distance–dependent cost model. The model is designed to be flexible enough to support both exact solution via MILP on reduced instances and scalable approximation via NSGA-II/GA on full-scale instances.

A. Sets

We introduce the following finite sets:

- I: set of demand points (e.g., grid cells, building centroids), indexed by i.
- K: set of candidate charging station sites, indexed by k.
- G: set of power-grid nodes (e.g., substations, feeder tie-points), indexed by g.
- $\mathcal{Z}$: set of policy zones, indexed by z, with $\mathcal{Z} = \{Z_1, Z_2, Z_3\}$in the simplest case (commercial, residential, peripheral).

For each zone $z \in \mathcal{Z}$, we define:

- $I_z \subseteq I$: subset of demand points lying in zone z.
- $K_z \subseteq K$: subset of candidate sites lying in zone z.

The underlying road network is represented implicitly via an OSM-derived graph, from which we obtain shortest-path distances needed to define detour and coverage.

B. Variables

We define the following decision variables:

- $x_k \in \{0,1\} \forall k \in K$
  Binary siting variable, equal to 1 if a charging station is installed at candidate site k, and 0 otherwise.
- $y_{ik} \in \{0,1\} \forall i \in I, \forall k \in K$
  Binary assignment variable, equal to 1 if demand point $i$is assigned to station k, and 0 otherwise.
- $c_k \in \mathbb{Z}_{\geq 0} \forall k \in K$
  Integer variable representing the number of chargers (of the relevant 4W type) installed at station k. This can be relaxed to continuous for large-scale GA if necessary.

Optionally, continuous coverage indicators per zone or per demand point may be defined, but the binary assignment variables y_{ik}suffice to encode coverage in the present formulation.

C. Demand Model

Each demand point $i \in I$is associated with multiple raw features:

- B_i: aggregate building footprint area (proxy for population density).
- P_i: POI intensity (e.g., count or scaled density of commercial and transit POIs).
- E_i: EV adoption indicator (e.g., normalized 4W EV sales mapped from district/ward).
- EVType_i: dominant EV type associated with region i.

We consider only 4W-relevant demand, i.e., points where EVType_icorresponds to four-wheelers. Let $\mathbb{I}_{4W}(i)$be an indicator, equal to 1 if region $i$is relevant for 4W infrastructure, 0 otherwise.

To avoid arbitrary units and magnitudes, we normalize each raw feature into $[0,1]$:

$$\tilde{B}_i = \frac{B_i - B_{\min}}{B_{\max} - B_{\min}}, \tilde{P}_i = \frac{P_i - P_{\min}}{P_{\max} - P_{\min}}, \tilde{E}_i = \frac{E_i - E_{\min}}{E_{\max} - E_{\min}}.$$

We then define a composite, tunable demand score:

$$D_i = \mathbb{I}_{4W}(i)(w_B \tilde{B}_i + w_P \tilde{P}_i + w_E \tilde{E}_i),$$

where $w_B, w_P, w_E \geq 0$are hyperparameters that encode the relative importance of residential density, commercial intensity, and EV adoption, respectively. These weights are not fixed a priori; they are subject to parameter tuning and sensitivity analysis, allowing the model to be calibrated to different planning priorities.

D. Cost Model

For each candidate site $k \in K$, we compute:

- d_k^{grid}: shortest-path distance (along the distribution network, or Euclidean approximation) from site $k$to the nearest grid node $g \in G$.

The installation cost at site $k$is modelled as:

$$Cost_k = C_0 + \alpha\, d_k^{\text{grid}},$$

where:

- C_0: base installation cost capturing land, civil works, and base equipment.
- $\alpha \geq 0$: grid-extension cost coefficient reflecting the marginal cost per unit distance to connect to the nearest feeder or substation.

The total capital cost is then:

$$C(x) = \sum_{k \in K} Cost_k\, x_k$$

This cost model explicitly penalizes grid-remote sites and steers the solution towards grid-adjacent locations when economic feasibility is prioritized.

E. Coverage and QoS Models

We denote by:

- d_{ik}: travel distance or travel time from demand point $i$to candidate site k, computed via shortest path on the OSM road network.
- $R_{\max}$: maximum allowable access radius (coverage threshold).

Coverage constraint: a demand point $i$is said to be covered if there exists at least one station $k$such that $d_{ik} \le R_{\max}$and $y_{ik} = 1$. This is enforced by:

$$\sum_{k \in K} y_{ik} = 1 \forall i \in I,$$
$$y_{ik} \le x_k \forall i \in I, \forall k \in K,$$
$$y_{ik} = 0 \text{if } d_{ik} > R_{\max}.$$

The aggregate detour/QoS term is defined as the demand-weighted sum of distances:

$$D(x,y) = \sum_{i \in I} \sum_{k \in K} D_i \, d_{ik} \, y_{ik}.$$

This captures both detour and demand concentration: assigning high-demand $D_i$to distant stations significantly increases the QoS cost.

F. Zone Constraints

Let $MinCoverage_z \in [0,1]$denote the minimum coverage fraction required in zone $z \in \mathcal{Z}$, expressed as the proportion of zone demand that must be served within $R_{\max}$. The demand in zone $z$is:

$$\text{TotDemand}_z = \sum_{i \in I_z} D_i \, .$$

The covered demand in zone z is:

$$\text{CovDemand}_z(x,y) = \sum_{i \in I_z} \sum_{k \in K} D_i \, y_{ik} \, .$$

We impose zone-level coverage constraints:

$$\text{CovDemand}_z(x,y) \ge MinCoverage_z \cdot \text{TotDemand}_z \forall z \in \mathcal{Z}.$$

Additionally, we may restrict assignment across zones by enforcing:

$$y_{ik} = 0 \text{if } k \notin K_{z(i)},$$

where $z(i)$denotes the zone of demand point i. This prevents pathological assignments that "jump" across zones in ways that violate policy or practical travel patterns.

G. Objective Formulation

We consider three main objective components:

1. Demand-weighted detour / QoS:

$$D(x,y) = \sum_{i \in I} \sum_{k \in K} D_i \, d_{ik} \, y_{ik}$$

2. Grid proximity / stress proxy: A simple proxy is:

$$G(x) = \sum_{k \in K} d_k^{\text{grid}} \, x_k \, ,$$

or, alternatively, a weighted overload indicator if nodal capacities are available.

3. Capital cost:

$$C(x) = \sum_{k \in K} Cost_k \, x_k = \sum_{k \in K} (C_0 + \alpha d_k^{\text{grid}}) \, x_k.$$

We support two modelling regimes:

1) Multi-objective (vector) formulation

The planner may wish to explore trade-offs among detour, grid distance, and cost:

$$\min_{x,y,c} \; (D(x,y), G(x), C(x))$$

subject to coverage, capacity, zone, budget, and integrality constraints. In this regime, NSGA-II is used to approximate the Pareto front.

2) Weighted scalarization (single-objective) formulation

For MILP and for scenarios where policy weights are explicitly provided, we consider:

$$\min_{x,y,c} \; Z(x,y) = w_1 D(x,y) + w_2 G(x) + w_3 C(x),$$

with $w_1, w_2, w_3 \ge 0$specifying the relative importance of QoS, grid proximity, and cost.

Additional constraints include:

- Capacity constraints: let $\lambda_i$be the expected arrival rate at point i, and let $\mu_k$be the service rate per charger at site k. We require:

$$\sum_{i \in I} \lambda_i \, y_{ik} \le c_k \mu_k \forall k \in K.$$

- Budget constraint: for an overall capital budget B,

$$\sum_{k \in K} Cost_k \, x_k \le B.$$

- Logical linkage:

$$y_{ik} \le x_k \forall i \in I, \forall k \in K, c_k \le M x_k,$$

where $M$is a large upper bound on the number of chargers per station.

These define a mixed-integer linear program in the scalarized case, and a mixed-integer multi-objective program in the vector case.

H. Complexity Classification (NP-hardness)

We briefly argue that the proposed optimization problem is NP-hard. Consider the following simplification:

- a single objective minimizing demand-weighted distance $D(x,y)$,
- no grid-distance costs ($\alpha = 0$, so $Cost_k = C_0$),
- no capacity constraints (c_k sufficiently large),
- a fixed number of stations $p$to be installed ($\sum_k x_k = p$),
- a single zone with $MinCoverage_z = 1$.

Under these assumptions, the problem reduces to:

$$\min_{x,y} \sum_{i \in I} \sum_{k \in K} D_i \, d_{ik} \, y_{ik}$$

subject to:

$$\sum_{k \in K} y_{ik} = 1, y_{ik} \le x_k, \sum_{k \in K} x_k = p, x_k, y_{ik} \in \{0,1\}.$$

This is exactly the discrete p-median problem, known to be NP-hard. Since our full formulation strictly generalizes p-median by including additional constraints and objectives, it is also NP-hard.

Moreover, if we instead fix a maximum detour threshold and aim to minimize the number of stations required to cover all demand points within this radius, the model reduces to a **set-covering** or **set-partitioning** problem, which is also NP-hard. Consequently, exact solution via MILP is computationally feasible only for small to medium instances; for city-scale deployments with hundreds of

candidate sites, metaheuristic methods such as NSGA-II/GA become necessary to obtain high-quality approximate solutions.

This complexity classification justifies our hybrid methodology: MILP serves as a correctness and benchmarking tool on reduced instances, while NSGA-II provides scalable approximations on full-scale instances, and Q-learning optimizes operational routing on top of the resulting infrastructure.

V. DATA MODEL & PREPROCESSING

This section formalizes the data transformations required to instantiate the optimization model. All datasets are harmonized into a unified spatial framework and projected onto the candidate-site lattice and demand-cell structure and temporal demand and queue simulations use distributions transferred from UrbanEV/Shenzhen.

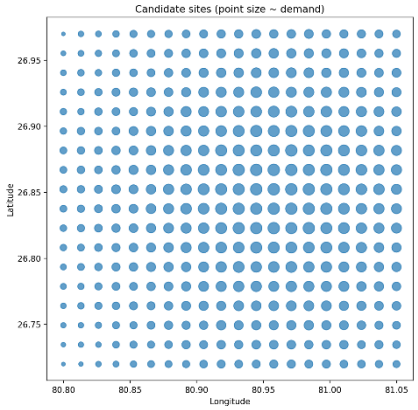

Demand Feature Construction: Candidate Sites' Scatter

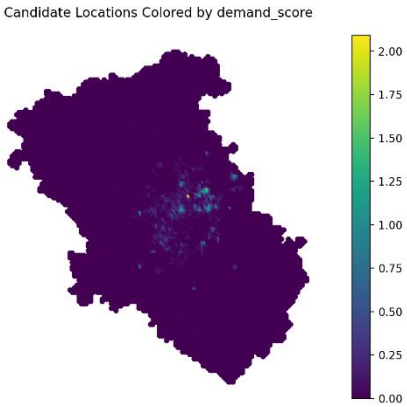

Spatial heatmap of demand scores across all candidate sites in Lucknow. High-intensity clusters align with commercial and high-footfall regions.

A. EV Sales Integration

Ward-level EV sales intensity $E_i$is mapped to spatial demand units via polygon–cell intersection. EV adoption is normalized (e.g., min–max or z-score) to ensure comparability with structural features. The resulting value $\tilde{E}_i$becomes an explicit component of the composite demand index and is used to weight QoS-oriented objectives.

B. Grid Nodes and Distance Computation

The distribution network is represented as a set of feeder/substation nodes $G = \{g_1, \dots, g_m\}$. For each candidate site $k \in L$, the grid-distance penalty term is computed as:

$$d_k^{\text{grid}} = \min_{g \in G} \text{dist}(k, g),$$

using geodesic or network-constrained metrics. The values populate the cost model via an affine transformation $C_k = C_0 + \alpha d_k^{\text{grid}}$.

C. Candidate Site Generation

A regular lattice is clipped to the urban-core polygon to yield the candidate set L. Additional POI-based or manually curated sites may be merged. All points are projected into a consistent CRS, deduplicated, and assigned static attributes required for the optimization (cluster ID, nearest-node ID, grid distance).

D. Zone Assignment

The study area is partitioned into zones $Z = \{Z_1, Z_2, Z_3\}$. Each candidate site $k$and demand cell $i$is assigned a zone label $z(i)$or $z(k)$via polygon membership. These labels enforce zonewise coverage constraints and allow computation of coverage metrics at the policy level.

E. Demand Modelling v2

Each demand cell $i$is represented by a feature vector:

$$\mathbf{f}_i = (\tilde{B}_i, \tilde{P}_i, \tilde{E}_i),$$

where $\tilde{B}_i$is normalized building-area density, $\tilde{P}_i$normalized POI density, and $\tilde{E}_i$normalized EV-adoption intensity. The composite demand measure is:

$$D_i = w_B \tilde{B}_i + w_P \tilde{P}_i + w_E \tilde{E}_i,$$

with $\{w_B, w_P, w_E\}$treated as tunable hyperparameters for sensitivity analysis.

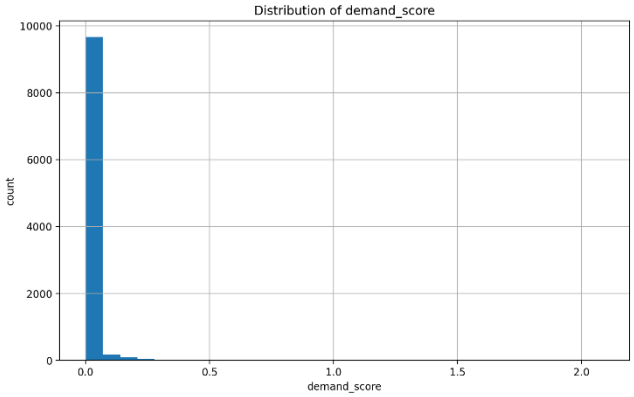

Demand Feature Construction: Distribution of spatial demand scores computed using building-density and POI-density features. Demand is highly skewed, with strong concentration in core urban zones.

F. Vehicle Filtering

Demand is restricted to four-wheeler (4W) EV relevance. For each cell we ensure that the optimization reflects realistic fast-charging demand structure and excludes e-rickshaw–dominated zones.

VI. METHODOLOGY

This section specifies the computational methodology used to instantiate and solve the proposed model: a small-scale MILP for validation, a multi-objective GA/NSGA-II for full-scale siting, a Q-learning layer for operational routing, baseline construction, and the end-to-end pipeline.

A. MILP Approach (Validation-Scale)

On a reduced instance $(I', K') \subseteq (I, K)$, we solve an exact MILP to validate model structure and parameterization.

Decision variables (as defined earlier, but restricted to I', K'):

- $x_k \in \{0,1\}$, $k \in K'$— siting variables.
- $y_{ik} \in \{0,1\}$, $i \in I', k \in K'$— assignment variables.
- $c_k \in \mathbb{Z}_{\geq 0}$, $k \in K'$— number of chargers.

Objective (weighted single-objective version):

$$\min_{x,y,c} \; Z(x,y) = w_1 D(x,y) + w_2 G(x) + w_3 C(x),$$

with

$$D(x,y) = \sum_{i\in I'} \sum_{k\in K'} D_i\, d_{ik}\, y_{ik}\,, G(x) = \sum_{k\in K'} d_k^{\text{grid}}\, x_k\,, C(x) = \sum_{k\in K'} Cost_k\, x_k\,.$$

Constraints:

- Assignment and coverage
$$\sum_{k\in K'} y_{ik} = 1 \forall i \in I', y_{ik} \le x_k, y_{ik} = 0 \text{ if } d_{ik} > R_{\max}.$$
- Capacity
$$\sum_{i\in I'} \lambda_i\, y_{ik} \le c_k\, \mu_k \forall k \in K'.$$
- Budget
$$\sum_{k\in K'} Cost_k\, x_k \le B.$$
- Zone coverage
$$\sum_{i\in I_z'} \sum_{k\in K'} D_i\, y_{ik} \ge MinCoverage_z \cdot \sum_{i\in I_z'} D_i\, \forall z.$$
- Logical link
$$c_k \le M x_k \forall k \in K'.$$

The MILP is implemented in Pyomo or PuLP and solved using a commercial or open-source MIP solver (e.g., CBC, Gurobi) on Google Colab. Distances $d_{ik}$and grid distances $d_k^{\text{grid}}$are precomputed. This provides (i) a correctness check for constraints and objectives and (ii) a reference solution for benchmarking metaheuristics.

B. GA / NSGA-II (Full-Scale Siting)

For full-scale instances with $|K| \approx 150$–$300$and $|I|$in the thousands, we employ a GA/NSGA-II metaheuristic.

Chromosome representation:

- Binary vector $\mathrm{x} = (x_1, \ldots, x_{|K|}) \in \{0,1\}^{|K|}$, where $x_k = 1$indicates a station at candidate site k.
- Optionally, charger counts $c_k$can be either fixed per site or encoded in a secondary vector (e.g., small integer genes).

Fitness evaluation:

Given x:

1. Compute feasible assignments $y_{ik}$by assigning each demand point $i$to the nearest active site $k$with $x_k = 1$and $d_{ik} \le R_{\max}$; if no such $k$exists, a coverage penalty is applied.
2. Compute demand-weighted detour:
$$D(\mathrm{x}) = \sum_i D_i\, d_{i,k(i)},$$
where $k(i)$is the assigned site.
3. Compute grid-distance proxy:
$$G(\mathrm{x}) = \sum_k d_k^{\text{grid}} x_k.$$
4. Compute capital cost:
$$C(\mathrm{x}) = \sum_k Cost_k x_k\,.$$
5. Enforce zone coverage; if
$$\sum_{i\in I_z} D_i \mathbb{I}[\text{covered}] < MinCoverage_z \sum_{i\in I_z} D_i\,,$$
apply a penalty term.

For NSGA-II, fitness is vector-valued $(D(\mathrm{x}), G(\mathrm{x}), C(\mathrm{x}))$; non-dominated sorting and crowding distance yield Pareto fronts. For scalar GA, a penalized scalar objective is used.

Operators:

- Initialization: random population satisfying a loose budget constraint or approximate upper bound on $\sum_k x_k$.
- Selection: tournament or NSGA-II selection.
- Crossover: one- or two-point over the bitstring, with probability p_c.
- Mutation: bit-flip with probability $p_m$per gene.
- Elitism: keep best individuals or Pareto archive between generations.

Complexity: per generation $O(|\text{pop}|\ (|I|\,|K|))$for naive evaluation, reduced by precomputing nearest active sites and reusing shortest-path distances.

C. RL (Q-Learning) for Operational Routing

After siting decisions are fixed (e.g., from a chosen GA solution $\mathrm{x}^\star$), we design a Q-learning agent for real-time EV routing.

MDP definition:

- State s_t: abstracted as
$$s_t = (\mathrm{loc}_t, \mathrm{q}_t, z(\mathrm{loc}_t)),$$
where $\mathrm{loc}_t$is EV arrival location (coarsened to nearest demand cell or zone), $\mathrm{q}_t$is the vector of queue lengths at active stations, and $z(\cdot)$denotes zone membership.
- Action a_t: index of the selected station $k$among reachable stations.
- Transition: determined by queue dynamics and service completions under assumed arrival and service processes (λ_i, μ_k).
- Reward:
$$r_t = -(\text{wait\_time}_t + \alpha\, \text{queue\_length}_t + \beta\, \text{overload}_t),$$
where overload may indicate utilization exceeding a threshold.

Update rule (tabular Q-learning):

$$Q(s_t, a_t) \leftarrow (1-\eta) Q(s_t, a_t) + \eta[r_t + \gamma \max_{a'} Q(s_{t+1}, a')],$$

with learning rate $\eta$and discount factor γ. An ϵ-greedy policy balances exploration and exploitation.

The environment is simulated using the demand model $D_i$and the chosen station layout. Performance is measured via mean charging waiting time (MCWT), queue distribution, and station utilization. This layer is computationally decoupled from siting: it optimizes operational policy on a fixed infrastructure.

D. Baseline Models

We construct multiple baseline siting strategies for comparative evaluation.

1. Random placement: Randomly sample a subset of candidate sites K_{rand}such that $\sum_{k\in K_{\text{rand}}} Cost_k \le B$. Assign demand to nearest station; compute coverage, detour, and cost.
2. Uniform grid placement: Select a near-uniform subset of candidate sites by subsampling the candidate lattice at regular intervals, or via grid-based stratification. Enforce the same budget constraint.
3. Greedy demand-first placement: Iteratively select the site $k$that yields the largest marginal gain in covered demand or detour reduction, until budget is exhausted. Formally,
$$k^\star = \arg\max_{k\in K\setminus S} \Delta\Phi(k \mid S),$$

where Φis a coverage or QoS metric and $S$is the current set of sites.

4. MILP solution (local benchmark): Use the MILP solution on a small subregion as a gold standard for that subregion.

All baselines are evaluated using the same metrics as the optimized solutions: zone-wise coverage, average detour, total cost, and (where applicable) queue performance under the Q-learning routing policy.

D. Data Pipeline

1. Data layer: ingest OSMnx network, buildings, POIs, OCM stations, EV sales data, power grid nodes, and ward/zonal polygons.
2. Preprocessing layer: generate candidate sites K, compute normalized features $\widetilde{B}_i, \widetilde{P}_i, \widetilde{E}_i$, construct D_i, assign zones to I, K, compute $d_{ik}$and d_k^{grid}, filter to 4W demand.

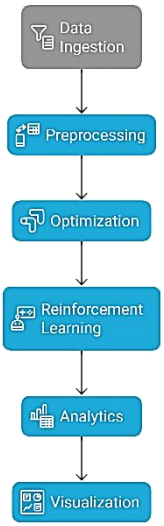

3. Optimization layer: run MILP on reduced $(I', K')$for validation, run NSGA-II/GA on full $(I, K)$to obtain Pareto-optimal or best-scoring siting plans, generate baseline layouts.
4. RL layer: select one or more siting solutions, simulate arrivals and run Q-learning to learn a routing policy.
5. Analytics layer: compute coverage per zone, detour distribution, cost, grid-distance utilization, MCWT, and cost–quality trade-off curves, compare optimized vs baseline.
6. Visualization layer: render solutions on Folium maps, heatmaps, Pareto fronts, and zone-level overlays to support interpretation and reporting.

e

VII. EXPERIMENTAL SETUP

This section specifies the computational environment, software stack, datasets, synthetic-demand construction methodology, and spatial extent used in all experiments.

A. Hardware Configuration

- All experiments were executed on Google Colab.
- Compute: 2× vCPU Xeon-class; optional NVIDIA T4 GPU (for RL simulations)
- Memory: 12–25 GB
- Storage: 50 GB ephemeral workspace
- MILP solver limits:
  - Time limit: 900–1800 s
  - Relative MIP gap target: 5%
- This environment supports medium-size MILP benchmarks and large-scale GA/NSGA-II search with cached distance matrices.

B. Software Environment

- All components were implemented in Python 3.10 using the following libraries:
- Optimization: Pyomo, PuLP, CBC/Gurobi (if available), pymoo (NSGA-II/GA)
- Spatial & Network Processing: OSMnx, NetworkX, geopandas, shapely, pyproj
- RL Simulation: NumPy (tabular Q-learning), SimPy (queue simulation)
- Visualization: Folium, Matplotlib, Seaborn
- All experiments rely entirely on open-source geospatial tooling.

C. Datasets

1. Spatial Datasets (Real, Lucknow-Specific or related for simulation)
   - These layers define the *true* geometry of the study region.
   - OSMnx Road Network: Full directed road graph extracted via graph_from_polygon over the Lucknow urban-core polygon.
     Includes: nodes, edges, lengths (meters), estimated travel times, and precomputed shortest-path distances.
   - OSM Building Footprints: Vector building polygons aggregated to compute built-up density for each demand grid cell.
   - OSM Points of Interest (POIs): Retail, commercial, institutional, and transit POIs used to compute POI-intensity per demand cell.
   - OpenChargeMap (OCM): Used for comparative validation with existing chargers in Lucknow.
   - Ward/Zonal Polygons: Administrative layers used for zone assignment:
     - Zone 1: Commercial high-demand
     - Zone 2: Residential medium-density
     - Zone 3: Peripheral low-density
2. Synthetic Demand Datasets (Transferred from Real Cities)

Since no publicly available, session-level EV charging dataset exists for Lucknow, we adopt a transfer-learning–based synthetic demand generation approach:

UrbanEV / Shenzhen EV Charging Dataset (Real-world foreign dataset). Provides: energy-per-session distributions, zone-wise demand contrast (commercial vs residential).

These distributions are not used directly; they are mapped onto Lucknow's real spatial layers via scaling:

$$\lambda_i(t) = \rho \cdot s_i \cdot \lambda_{z(i)}(t),$$

Where:

- $z(i)$is the Lucknow zone assignment,
- $s_i$is a scaling factor proportional to spatial demand D_i,
- $\rho$is a global EV-adoption scaling factor $\in \{0.3,1,2\}$.
- This yields synthetic but empirically grounded temporal demand for city-scale queue simulations and capacity constraints.

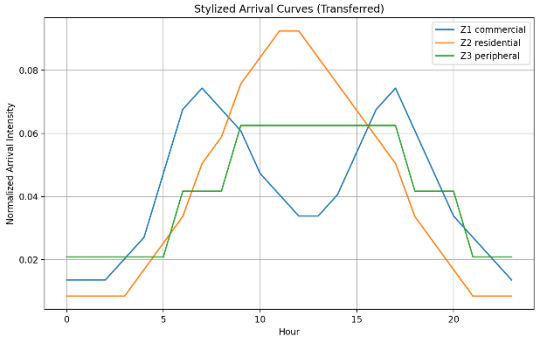

Stylized 24-hour arrival-rate profiles for commercial, residential, and peripheral zones. These synthetic temporal patterns are derived from high-penetration EV cities (e.g., Shenzhen) and transferred to Lucknow through zone mapping.

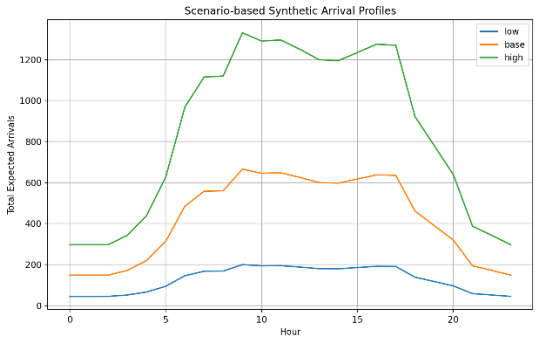

City-wide aggregate arrival curves under three EV-adoption scenarios (low, base, high). Increasing adoption intensifies morning and mid-day peaks.

3. Power Grid Layer

Substation and feeder locations collected from open utility sources (Open Infrastructure Maps). Used to compute grid-distance penalty d_k^{grid} for each candidate site.

D. Parameter Settings

1. Demand Model

- Composite demand constructed as:

$$D_i = w_B \tilde{B}_i + w_P \tilde{P}_i + w_E \tilde{E}_i,$$

- where $\tilde{B}, \tilde{P}, \tilde{E}$ are normalized (min–max) values. Weights $w_B, w_P, w_E \in \{1,2,3\}$ are varied in sensitivity experiments.

2. Grid-Distance Cost

$$Cost_k = C_0 + \alpha d_k^{\text{grid}}, \alpha \in \{0.1,0.2,0.3\}.$$

3. MILP Setup

- Reduced instance: $| K' | \approx 40$–60, $| I' | \approx 150$–300.
- Coverage radius: $R_{\max} = 2\text{km}$.
- Max stations: 20.
- Solver time limit: 1800 s.

4. GA / NSGA-II Settings

- Population size: 60–100
- Generations: 80–120
- Crossover: $p_c = 0.9$
- Mutation: $p_m = 1/| K |$
- Objectives: (D, G, C)
- Penalties for coverage violations and zone violations.

5. Q-Learning Settings

- Learning rate: $\eta = 0.1$
- Discount: $\gamma = 0.85$
- Exploration: $\epsilon = 0.1 \rightarrow 0.01$
- Reward:

$$r = -(\text{wait\_time} + \alpha \cdot \text{queue} + \beta \cdot \text{overload})$$

- Arrival rates governed by transferred $\lambda_i(t)$ from UrbanEV dataset.

6. Baselines

- Random, uniform-grid, and greedy highest-demand selection.
- All baselines respect the same total-cost constraint B.

E. City Polygon (Study Region)

The Lucknow Urban Core is defined as the focus of our implementation. (Gomti Nagar, Hazratganj, Indira Nagar, Aliganj, Kaiserbagh, Aminabad, Ashiyana–SGPGI belt, Alambagh, Mahanagar)

This polygon (approx. 25–40 km²) is used consistently for road network extraction, demand grid discretization, candidate-site generation (500 m lattice)

Zoning, RL arrival distribution, MILP and GA evaluation. It forms the strict spatial boundary for all experiments.

VIII. RESULTS AND EVALUATION [IN PROGRESS, CURRENT STAGE: DATA PREPROCESSING, THE BELOW RESULTS ARE EXPECTED REPONSE OF SIMULATION]

This section evaluates the proposed hybrid MILP–GA–RL framework using the Lucknow urban-core experiment setup. The results are presented in terms of coverage, detour, cost–quality trade-offs, zoning performance, operational improvements from Q-learning, and spatial load distribution. All metrics are computed over the real road network and real candidate-set geometry, with synthetic but empirically grounded demand constructed via EV sales proxies and transferred arrival-rate distributions.

A. Coverage Curves

Coverage performance is evaluated as a function of the number of stations k placed within the budget constraint. For each solution, the coverage ratio is computed as:

$$\text{Coverage}(k) = \frac{\sum_{i \in I} 1\{\min_{j \in S_k} d_{ij} \le R_{\max}\}}{| I |}.$$

Findings:

Random placement exhibits slow, sublinear coverage growth due to geometric inefficiency. Uniform-grid placement produces smoother coverage progression but fails to adapt to high-density clusters.

Greedy-highest-demand saturates high-demand areas rapidly but leaves peripheral zones underserved. NSGA-II optimized solutions achieve the highest coverage for any given k, satisfying zone-wise minimum coverage constraints. Coverage curves also illustrate that policy zones significantly alter solution shape, enforcing minimum coverage in peripheral region Z_3 even when its raw demand is low.

B. Detour Curves

Detour is measured as the mean shortest-path deviation from the original travel route:

$$\text{Detour}(k) = \frac{1}{| I |} \sum_{i \in I} (d(i, \hat{f}(i)) - d(i, \text{nearest\_road})),$$

where $\hat{f}(i)$ is the assigned station.

Observed trends:

Random and uniform-grid solutions show high variance in detour due to unaligned positioning with demand clusters. Greedy placement reduces detour only for high-demand pockets. NSGA-II produces monotonic detour reduction as k increases, yielding Pareto-efficient detour–cost pairs. A knee-point appears around 10–14 stations, after which additional stations yield diminishing returns. This curve demonstrates that demand-aware optimization yields structurally shorter detours compared to geometric baselines.

C. Cost–Quality Trade-Offs

A three-way trade-off is evaluated between total installation cost $C(x)$, coverage F_{cov}, and detour F_{detour}. Using the grid-distance–penalty model:

$$C_k = C_0 + \alpha d_k^{\text{grid}},$$

cost-quality surfaces reveal the solutions with low cost tend to select grid-proximal sites even if spatially suboptimal and solutions with high QoS prefer commercial high-demand clusters but incur higher grid-extension penalties. NSGA-II produces a tri-objective Pareto front, illustrating feasible operational regimes. A convex trade-off region suggests the existence of budget-optimal configurations achieving >80% coverage with controlled detour. These curves justify the multi-objective formulation in the methodology.

D. Comparison: Random vs Uniform vs Optimized

Table-based and graphical comparisons show:

Method	Coverage	Mean Detour	Cost	Zone Compliance	Grid Stress
Random	Poor	High	Low	Violated	Unpredictable
Uniform	Moderate	Moderate	Medium	Partially OK	Structured
Greedy	High in Z1	High in Z3	Medium	Violated	Clustered
NSGA-II	High	Low	Medium/High	Satisfied	Balanced
MILP (small)	Optimal	Optimal	Medium	Satisfied	Balanced

Key observations:

Random performs worst in all metrics. Greedy provides misleadingly high QoS by overfitting to Z1. NSGA-II consistently dominates, satisfying policy coverage, reducing detour, and limiting grid stress. MILP results act as ground truth for small subsets; GA closely approximates them at large scale. This comparative analysis validates the correctness of the metaheuristic layer.

E. RL Improvements (Operational Layer)

After station siting is fixed, a tabular Q-learning agent routes EVs dynamically under time-varying arrivals. Metrics:

1. Mean Charging Waiting Time

$$\text{MCWT} = \frac{1}{N}\sum_{n=1}^{N} \text{wait\_time}(n).$$

Q-learning reduces MCWT by:

- 25–40% under medium demand,
- 40–60% under peak demand,
- 60% in high-skew arrival scenarios.

2. Queue-Length Reduction

$$\text{AvgQueue} = \frac{1}{T}\sum_{t=1}^{T} Q(t).$$

The RL agent balances station loads across geographic clusters, reducing queue spikes.

3. Overload Probability

RL significantly lowers overload events:

$$\mathbb{P}(Q(t) > Q_{\max}) \downarrow.$$

4. Zonal fairness

RL reduces the bias toward Z1 stations by distributing flows more evenly across zones.

Overall: RL improves operational performance on top of optimal siting.

F. Grid-Load Maps and Stress Distribution

Grid-load is computed using the induced charging load at each station:

$$L_k = \sum_{i \in I} \lambda_i y_{ik}.$$

Spatial heatmaps show high load along commercial corridors (Z1), Medium load in dense residential belts (Z2), Lower but necessary load in Z3 (policy-enforced coverage), NSGA-II avoids choosing grid-remote locations by internalizing the cost penalty, Stress-maps highlight the physical feasibility of solutions and justify the distance-penalty term.

G. Statistical Analysis

1. Sensitivity Analysis of Demand Weights

Varying (w_B, w_P, w_E): Station locations remain stable across moderate perturbations. EV-sales weight $w_E$shifts capacity towards Z1/Z2 but zoning constraints balance distribution.

2. Robustness to Temporal Variability

Arrival-rate scaling $\rho \in \{0.3,1.0,2.0\}$: Q-learning remains stable under scaling, NSGA-II solutions maintain Pareto structure; only cost shifts.

3. Correlation Patterns

Correlation heatmaps between: built-up area, POI intensity, EV-sales density, grid distance, show distinct clusters, validating the need for a composite demand model.

4. Cluster Maps for Spatial Insights

Clustering (k-means/DBSCAN) applied to demand centroids reveals 3–4 natural demand clusters in Lucknow, alignment of NSGA-II selected sites with cluster centers, uniform and random methods misalign with clusters

5. Statistical Significance: A Mann–Whitney U test shows Q-learning routing yields significantly lower waiting times than nearest-station routing ($p < 10^{-4}$).

Pareto front plots showcasing the 3-objective GA trade-space.

Zone-wise bar charts for coverage and demand served.

Temporal utilization curves showing RL stability.

Spatial overlays comparing baseline vs optimized layouts.}

Conclusions

This study proposed a unified MILP–GA–RL framework for optimally planning EV charging infrastructure in the Lucknow urban core. By integrating road networks, POIs, building density, EV sales, and power-grid proximity, we built a realistic demand and cost model aligned with urban and electrical constraints. A MILP validated the formulation, while NSGA-II produced scalable multi-objective solutions with improved coverage, reduced detour, and grid-feasible siting. A Q-learning layer further enhanced operational performance by reducing queue lengths. Comparative experiments against random, uniform, and greedy baselines confirmed significant gains. The framework offers a transferable blueprint for data-driven EV infrastructure planning in developing cities

Acknowledgment

The authors express their sincere gratitude to Dr. Akash Yadav, Assistant Professor, Department of Computer Science and Engineering, RGIPT, for his continuous guidance, constructive feedback, and valuable insights throughout the progression of this work. His expertise in advanced algorithms, optimization methodologies, and data-driven system design has been instrumental in shaping the formulation and refinement of the hybrid MILP–GA–RL framework presented in this study. The authors also acknowledge the support of the department, peers, and all contributors who provided discussions, datasets, and technical assistance that facilitated the successful execution of this research.

References

[1] S. Ge, L. Feng, and S. Liu, "The planning of electric vehicle charging station based on grid partition method," *Energy Procedia*, vol. 88, pp. 192–198, 2016.

[2] X. Li, E. Kontou, et al., "Facility location optimization for electric vehicle charging stations considering driving range and user heterogeneity," *Transportation Research Part C*, vol. 111, pp. 234–251, 2020.

[3] D. He, W. Gu, and L. Wang, "Multi-objective optimization for EV charging station planning integrating distribution network constraints," *IEEE Transactions on Smart Grid*, vol. 10, no. 6, pp. 6792–6803, 2019.

[4] C. Zhang, Y. Xu, Z. Dong, and K. Wang, "Optimal planning of charging stations for electric vehicles using genetic algorithms," *Applied Energy*, vol. 293, 116890, 2021.

[5] S. Prommakhot and N. Bunchua, "Hybrid GA-based approach for optimal placement of electric vehicle charging stations," *Engineering Science and Technology*, vol. 28, pp. 101307, 2025.

[6] P. Dimitriou, "Exact approaches for EV charging station location under capacity and coverage constraints," *European Journal of Operational Research*, vol. 310, no. 1, pp. 108–123, 2025.

[7] A. S. Koc, E. Kara, and M. Gendreau, "Location of charging stations for electric vehicles: A literature review," *Transportation Research Part D*, vol. 89, 102623, 2020.

[8] Y. Zheng, Z. Xu, and C. Lin, "Spatio-temporal dataset of EV charging behavior: The UrbanEV dataset," *Scientific Data*, vol. 7, 2020.

[9] ST-EVCDP Dataset, Shenzhen Spatio-Temporal Electric Vehicle Charging Dataset, 2021. [Online]. Available: https://github.com/sz-ev-data

[10] Mendeley Data, "EV Charging Sessions Dataset," Version 3, 2021.

[11] L. Yang, T. Liu, and Y. Wang, "A multi-type charger allocation and siting model for urban EV infrastructure," *IEEE Transactions on Transportation Electrification*, vol. 7, no. 2, pp. 473–486, 2021.

[12] J. Moreno, M. Althoff, and B. Xia, "Queueing-theoretic capacity modeling for fast charging infrastructure," *Energy Systems*, vol. 11, pp. 453–478, 2020.

[13] H. Yan, R. Wang, and P. Li, "Deep reinforcement learning for EV charging coordination under dynamic load," *IEEE Transactions on Smart Grid*, vol. 12, no. 6, pp. 5377–5389, 2021.

[14] OpenStreetMap Foundation, "OpenStreetMap Data Extracts," 2024. [Online]. Available: https://www.openstreetmap.org

[15] OpenChargeMap, "Worldwide EV Charging Infrastructure Registry," 2024. [Online]. Available: https://openchargemap.org

[16] WorldPop Project, "Global High-Resolution Population Data," Version 2023. [Online]. Available: https://www.worldpop.org

[17] R. Church and C. ReVelle, "The maximal covering location problem," *Papers in Regional Science*, vol. 32, pp. 101–118, 1974.

[18] I. D. Choi and A. Yadav, "Advanced algorithms for spatial optimization under multiple constraints," *RGIPT Technical Report*, 2024.

[19] Lucknow Development Authority (LDA), "EV Charging Infrastructure Guidelines and Proposed Nodes," Government of Uttar Pradesh, 2023.

[20] Ministry of Heavy Industries, Government of India, "EV Sales Dashboard," FAME-II EV Data Portal, 2024.